NASA
Technical
Paper
2415
C.2
April 1985

Ignition of Mixtures of SiH_4, CH_4, O_2, and Ar or N_2 Behind Reflected Shock Waves

Allen G. McLain,
Casimir J. Jachimowski,
and R. Clayton Rogers

NASA

NASA Technical Paper 2415

1985

Ignition of Mixtures of SiH_4, CH_4, O_2, and Ar or N_2 Behind Reflected Shock Waves

Allen G. McLain,
Casimir J. Jachimowski,
and R. Clayton Rogers

Langley Research Center
Hampton, Virginia

NASA
National Aeronautics and Space Administration

Scientific and Technical Information Branch

Introduction

Subscale engine tests have demonstrated that silane is an effective combustion initiator for a proposed hydrogen-fueled supersonic combustion ramjet. Experiments performed in the Langley Hypersonic Propulsion Test Cells and in contractor facilities (refs. 1 and 2) indicate that silane promotes hydrogen ignition and also helps sustain combustion over a range of inlet combustor conditions. Subsequent experiments in the chemical kinetic shock tube at Langley Research Center (ref. 3) have yielded kinetic information about the silane-hydrogen oxidation mechanism through direct measurement of ignition delay times. The tests were performed at pressures and temperatures comparable with those experienced within a supersonic ramjet combustor. Theoretical ignition delay times were corrected by altering referenced kinetic coefficients within recommended error limits (see ref. 4) to improve agreement between theory and experiment. At the time of the studies of references 3 and 4, hydrogen ignition and hydrogen ignition enhancement in scramjets were of primary interest. Recently interest has focused on liquid-hydrocarbon-fueled interceptor-type missiles powered by supersonic combustion ramjet engines. An engine of this type requires fuel with a long storage time and high energy density. Such fuels are generally characterized by long ignition delay times and require some type of ignition aid and piloting. For this study, methane, the simplest hydrocarbon with the best characterized kinetic mechanism and thermochemical properties, was selected for ignition delay study in the chemical kinetic shock tube.

The purpose of this paper is to present the results of an ignition delay time study of methane-silane-oxygen-nitrogen and methane-silane-oxygen-argon mixtures and to compare experimental data with theoretical calculations based on a combined reaction mechanism. The results of reference 4 showed that the ignition behavior of silane-hydrogen mixtures can be predicted theoretically with a reasonable degree of accuracy.

Experimental Apparatus and Measurements

Ignition delay times were measured behind reflected shock waves in a stainless steel tube with an inside diameter of 8.9 cm. The driven section was 676.1 cm long. The only difference in hardware from the study of reference 3 was that the driven section was lengthened by 5.1 cm to accommodate a ring fixture with eight optical or pressure transducer ports 2.54 cm from the end plate of the shock tube. This arrangement, shown in figure 1, allows simultaneous pressure and optical measurements 2.54 cm upstream of the end plate. As in the previous study of silane-hydrogen ignition characteristics (ref. 3), ignition delay times were measured primarily with a pressure transducer located in the center of the end wall plate (i.e., on the axial centerline of the shock tube) with the sensing surface protruding 3 mm into the approaching shock wave and incoming flow.

The passage of the incident shock wave was detected by several pressure transducers at various stations along the driven section. The output from these transducers activated and stopped digital timers from which velocities along the tube were determined using the familiar time of arrival technique. The time constant for the pressure measurements was 4 μs $\pm$ 0.5 μs for the entire series of tests. This time constant is about the same time required for the shock wave to move from the front edge of a transducer sensing surface to the rear edge of a transducer sensing surface. The range in measured velocities for the test series resulted in incident shock wave Mach numbers ranging from 2 to 3.

All the instrumentation for determining shock velocity, pressure, and radiative emission was located over the last 176.1 cm of the driven section between a station 500 cm downstream of the diaphragm and the reflecting end plate. Measurements taken during this final length were examined to determine whether ignition occurred at the arrival of the incident shock wave. When ignition occurred at the shock wave arrival, test results were discarded. The time interval between the incident shock wave and the contact surface between the driven and driver gases was in excess of 2000 μs when the incident shock was 670 cm downstream of the diaphragm location.

The additional viewing port locations provided by the ring fixture shown in figure 1 allowed optical measurements to be made simultaneously at one axial location. These measurements were (1) the emission from CO_2 at 4.38 μm; (2) the emission from CO at 5.0 μm; and (3) the emission from the chemiluminescent reaction to form excited CO_2*, or the [O][CO] product, at 366 nm. For the optical measurements, the emission from the shocked gases passed through calcium fluoride windows and 16-cm-long slits, 1 mm wide and 6.34 mm high. For the measurement of CO_2 emission, the emissions from the slit entered a 0.25-m Ebert type, compact infrared monochromator. An indium antimonide (InSb), liquid-nitrogen-cooled detector at the exit of the monochromator was used to convert the emission to a voltage output suitable for recording with an oscilloscope. The radiation was centered at 4.38 μm by proper orientation of an internal 148 groove/mm grating blazed at 5.0 μm. For the measurement

of CO emission, the radiation from the slit-window arrangement passed through an interference filter centered at 5.0 μm with a half-bandwidth of 0.15 μm and was then measured with the same type of InSb infrared detector. The [O][CO] product (or excited CO_2*) chemiluminescent emission passing through the same slit-window arrangement was detected with a photomultiplier with a characteristic S-20 response. The interference filter used was centered at 366 nm with a bandwidth at half-peak of 6.5 nm. Any combination of these detectors could be used during an actual test. Both optical and pressure transducer measurements could be used to detect ignition.

The static pressure behind the reflected shock wave, p_5 was approximately 1.25 atm for all tests (i.e., for argon and nitrogen as the diluent gas and for different equivalence ratios). The diaphragm separating the driver and driven sections was 0.0075-mm-thick Mylar, which ruptured at a driver pressure of approximately 3.5 atm. Thus, to achieve a range of static temperature behind the reflected shock wave T_5 at a relatively constant pressure p_5, the speed of sound of the driver gas and initial pressure of the driven (test) gas p_1 was regulated. (As is well known for shock tubes, the initial driven gas pressure must be decreased as the incident shock wave velocity is increased to obtain a constant value of p_5.) The initial pressure p_1 ranged from 20 to 40 mm of mercury in the present study. The driver gas was a mixture of unheated helium and argon. By increasing the partial pressure of helium, thereby decreasing the molecular weight and increasing the speed of sound of the driver gas, a stronger incident shock wave was formed. Varying the driver gas speed of sound, the initial driven gas pressure, the diluent gas, and the equivalence ratio resulted in a range of T_5 from 1100 K to 1300 K.

Four gas mixtures were tested with overall equivalence ratios of 0.7 and 1.0 with either argon or nitrogen as the diluent. The compositions of these mixtures are presented in table I.

These mixtures were obtained by diluting a commercially supplied mixture of 20 mole-percent silane and 80 mole-percent methane with nitrogen or argon. The final mixture was accomplished by adding the oxygen to the diluted silane-methane mixture within the shock tube. This procedure prevented oxidation of the silane in the mixing bottle as described in reference 3. Briefly, methane, silane, and argon or nitrogen were premixed in a large stainless steel mixing vessel to a total pressure of 3.33 atm. This mixture was allowed to come to equilibrium over a period of several days. The desired mixture was achieved by adding the appropriate partial pressure of oxygen to the evacuated shock tube and then adding the premixed gases until the desired initial pressure in the driven section was obtained.

TABLE I. COMPOSITION OF GAS MIXTURES

(a) Overall equivalence ratio of 0.7

Species	Mole-percent
SiH_4	0.021
H_2	.084
O_2	.300
N_2 or Ar	.595

(b) Overall equivalence ratio of 1.0

Species	Mole-percent
SiH_4	0.021
H_2	.084
O_2	.210
N_2 or Ar	.685

Experimental Results and Data Analysis

An example of the pressure time histories behind both the incident shock wave and the reflected shock wave is shown in figure 2. Also shown in this figure are samples of optical sensor measurements. The lower trace (fig. 2(d)) is the pressure history for the transducer protruding 3 mm from the end (reflecting) plate on the axial centerline of the shock tube. The ignition delay time shown in this figure is approximately 750 μs for a pressure level of 1.25 atm with argon as the diluent gas. Upon flow arrival at the protruding pressure probe, the pressure sharply increased and then abrubtly decreased (within 5 μs) toward the expected value of pitot pressure in the region behind the incident shock. The sensor experienced this "overshoot" because a reflected shock wave was established at the probe tip upon arrival of the incident shock wave; this reflected wave formed at the face of the sensor adjusted to a standing shock in what is commonly referred to as the "flow establishment process." At about the time that the sensor signal began to level out, the reflected shock wave from the end plate of the tube passed the sensor; thus the sensor then detected the pressure behind the reflected shock, p_5. The trace in figure 2(c) is the voltage registered by the infrared detector monitoring emission from carbon dioxide. As can be seen from this trace, no emission from carbon dioxide was observed until approximately 1000 μs had passed. The time zero in this figure represents an arbitrary time when the recording equipment was started and should not

be confused with the zero for ignition delay time, which occurred after passage of the reflected wave. The significance of this late emission of carbon dioxide may be better understood by examining the tube wall pressure at the same axial location as the carbon dioxide detector. In this trace (fig. 2(b)), the first rise in pressure (noted at about 200 μs on the abscissa) corresponds to arrival of the incident shock wave. The next rise in pressure corresponds to arrival of the reflected shock wave. The dramatic rise in pressure toward the end of the trace indicates when ignition occurred at this location. Notice that carbon dioxide emission appeared at the same time as the ignition pressure rise at the tube wall. Also, the emission from carbon monoxide monitored at 5.0 μm and illustrated in the uppermost trace (fig. 2(a)) appeared at this same time.

In figure 3, emission and pressure at four radial positions at the same axial location are compared. No emission from the carbon-containing compounds was detected during the ignition delay period. At ignition, however, indicated by the pressure rise in the lower trace, radiation is clearly evident from carbon dioxide and carbon monoxide in the infrared region of the spectrum and from the atomic oxygen and carbon monoxide product (observed at 366 nm in the near-ultraviolet region of the spectrum). The experimental results of figures 2 and 3 show that silane and methane ignition occurred simultaneously (that is, within the time resolution of the measurement).

The measured ignition delay times are plotted against reciprocal temperature for argon and nitrogen as the diluents in figure 4 for an equivalence ratio of 0.7 and in figure 5 for an equivalence ratio of 1.0. In these figures, as in previous ignition delay time studies in the shock tube, the temperature behind the reflected shock wave T_5 represents the temperature of the mixture components in a frozen condition (i.e., the temperatures were calculated with the initial components unreacted in a true reflected shock case). Comparison of figures 4 and 5 indicates that equivalence ratio had very little effect on ignition delay. With argon as the diluent gas, the ignition delay times at the same temperatures were longer than with nitrogen as the diluent gas. This difference in ignition delay time may be partially attributed to a higher third body efficiency for nitrogen, since diatomic species, such as nitrogen, are generally more efficient as third body catalysts than monatomic species, such as argon. Also, nitrogen may not be totally inert in a reactive silicon system. Although there is no direct evidence that silicon-nitrogen reactions did occur, the residue in the shock tube following a test differed in color for the two diluent gases. The residue formed with argon as the diluent was dark gray, whereas the residue with nitrogen as the diluent was brown. The difference in ignition delay time for the two diluents is about the same for both equivalence ratios (figs. 4 and 5). The least squares curve fits to the data for an equivalence ratio of 0.7, shown in figure 4, yields

$$\tau = 3.95 \times 10^{-2}\, e^{11\,339/T_5}$$

for argon as the diluent gas, where τ is ignition delay time (in microseconds) and T_5 is temperature (Kelvin) behind the reflected shock; also

$$\tau = 6.83 \times 10^{-3}\, e^{12\,800/T_5}$$

for nitrogen as the diluent gas. The least squares curve fits to the data for an equivalence ratio of 1.0 (stoichiometric), shown in figure 5, yield

$$\tau = 1.0 \times 10^{-3}\, e^{15\,732/T_5}$$

for argon as the diluent and

$$\tau = 2.0 \times 10^{-4}\, e^{16\,944/T_5}$$

for nitrogen as the diluent gas.

Comparison of Experimental Results and Kinetic Model

The experimental ignition delay times were compared with analytic results obtained by using the silane-methane oxidation kinetic mechanism presented in table II and the silane oxidation mechanism presented in reference 4. The shock tube experiments were simulated with the chemical kinetic computer code described in reference 5. The code was operated in a constant density mode to simulate conditions behind the reflected shock wave. In these numerical experiments, the ignition delay time was defined to be the elapsed time between the heating of the gas mixture by the reflected shock wave and the sudden pressure increase due to combustion.

The silane-methane oxidation mechanism given in table II and used to perform the numerical studies is based on the mechanisms proposed in references 6 and 7. To test the adequacy of the mechanism for the experimental conditions in this study, the calculated ignition delay times were compared with an empirical curve fit of experimental data reported in reference 7 for a stoichiometric methane-oxygen mixture with a composition near that used in this study. The results of these calculations are shown in figure 6. The experimental and calculated results agree very well.

The good agreement between the methane kinetic mechanism and experimental results at nearly the

TABLE II. METHANE-SILANE REACTION MECHANISM

Reaction	*A	*n	*E
$M + CH_4 \rightarrow CH_3 + H + M$	1.00×10^{17}	0	85 800
$CH_4 + O_2 \rightarrow CH_3 + HO_2$	1.90×10^{11}	0	58 500
$CH_4 + HO_2 \rightarrow CH_3 + H_2O_2$	2.00×10^{13}	0	17 913
$H + CH_4 \rightarrow CH_3 + H_2$	7.23×10^{14}	0	15 060
$O + CH_4 \rightarrow CH_3 + OH$	4.10×10^{14}	0	13 970
$OH + CH_4 \rightarrow CH_3 + H_2O$	3.00×10^{13}	0	6 000
$CH_3 + O \rightarrow CH_2O + H$	1.30×10^{14}	0	2 000
$CH_3 + O_2 \rightarrow CH_3O + O$	2.50×10^{14}	0	29 000
$CH_3 + HO_2 \rightarrow CH_3O + OH$	1.60×10^{13}	0	0
$CH_3 + OH \rightarrow CH_2O + H_2$	4.00×10^{12}	0	0
$CH_3O + O_2 \rightarrow CH_2O + HO_2$	1.00×10^{12}	0	6 000
$M + CH_3O \rightarrow CH_2O + H + M$	5.00×10^{13}	0	21 000
$M + CH_2O \rightarrow HCO + H + M$	5.00×10^{16}	0	72 000
$H + CH_2O \rightarrow HCO + H_2$	3.30×10^{14}	0	10 500
$O + CH_2O \rightarrow HCO + OH$	1.80×10^{13}	0	3 100
$OH + CH_2O \rightarrow HCO + H_2O$	7.50×10^{12}	0	170
$CH_2O + HO_2 \rightarrow H_2O_2 + HCO$	1.26×10^{12}	0	8 000
$M + HCO \rightarrow H + CO + M$	5.00×10^{14}	0	19 000
$H + HCO \rightarrow CO + H_2$	2.00×10^{14}	0	0
$O + HCO \rightarrow CO + OH$	1.00×10^{14}	0	0
$OH + HCO \rightarrow CO + H_2O$	1.00×10^{14}	0	0
$O_2 + HCO \rightarrow CO + HO_2$	3.20×10^{12}	0	7 000
$OH + CO \rightarrow CO_2 + H$	1.68×10^{7}	1.3	-656
$M + CO + O \rightarrow CO_2 + M$	2.50×10^{15}	0	4 370
$SiH_4 \rightarrow SiH_2 + H_2$	3.30×10^{12}	0	51 090
$SiH_4 + O_2 \rightarrow SiH_3 + HO_2$	2.00×10^{11}	0	44 000
$SiH_4 + HO_2 \rightarrow SiH_3 + H_2O_2$	3.00×10^{12}	0	5 600
$SiH_4 + H \rightarrow SiH_3 + H_2$	1.50×10^{13}	0	2 500
$SiH_4 + O \rightarrow SiH_3 + OH$	4.20×10^{12}	0	1 600
$SiH_4 + OH \rightarrow SiH_3 + H_2O$	8.40×10^{12}	0	100
$H + SiH_3 \rightarrow SiH_2 + H_2$	1.50×10^{13}	0	2 500

*The parameters A, n, and E refer to the Arrhenius equation, $k = AT^n e^{-E/RT}$. The rate coefficient k is in s^{-1} for unimolecular reactions, cm^3/mole-s for bimolecular reactions, and cm^6/$mole^2$-s for termolecular reactions. Activation energy E is in cal/mole.

TABLE II. Concluded

Reaction	*A	*n	*E
$O + SiH_3 \rightarrow SiH_2O + H$	1.30×10^{14}	0	2 000
$OH + SiH_3 \rightarrow SiH_2O + H_2$	5.00×10^{12}	0	0
$SiH_3 + O_2 \rightarrow SiH_2O + OH$	8.60×10^{14}	0	11 430
$SiH_2 + O_2 \rightarrow HSiO + OH$	1.00×10^{14}	0	3 700
$M + SiH_2O \rightarrow HSiO + H + M$	5.00×10^{16}	0	76 600
$SiH_2O + H \rightarrow HSiO + H_2$	3.30×10^{14}	0	10 500
$SiH_2O + O \rightarrow HSiO + OH$	1.80×10^{13}	0	3 080
$SiH_2O + OH \rightarrow HSiO + H_2O$	7.50×10^{12}	0	170
$SiH_2O + HO_2 \rightarrow HSiO + H_2O_2$	1.00×10^{12}	0	8 000
$M + HSiO \rightarrow SiO + H + M$	5.00×10^{14}	0	29 000
$HSiO + H \rightarrow SiO + H_2$	2.00×10^{14}	0	0
$HSiO + O \rightarrow SiO + OH$	1.00×10^{14}	0	0
$HSiO + OH \rightarrow SiO + H_2O$	1.00×10^{14}	0	0
$HSiO + O_2 \rightarrow SiO + HO_2$	1.20×10^{14}	0	3 975
$SiO + OH \rightarrow SiO_2 + H$	4.00×10^{12}	0	5 700
$M + SiO + O \rightarrow SiO_2 + M$	2.50×10^{15}	0	4 370
$SiO + O_2 \rightarrow SiO_2 + O$	1.00×10^{13}	0	6 500
$H + O_2 \rightarrow OH + O$	1.42×10^{14}	0	16 400
$OH + H_2 \rightarrow H_2O + H$	3.16×10^{7}	1.8	3 030
$O + H_2 \rightarrow OH + H$	2.07×10^{14}	0	13 750
$OH + OH \rightarrow H_2O + O$	5.50×10^{13}	0	7 000
$M + H + OH \rightarrow H_2O + M$	2.21×10^{22}	−2	0
$M + H + H \rightarrow H_2 + M$	6.53×10^{17}	−1	0
$M + H + O_2 \rightarrow HO_2 + M$	3.20×10^{18}	−1	0
$HO_2 + OH \rightarrow H_2O + O_2$	5.00×10^{13}	0	0
$HO_2 + H \rightarrow H_2 + O_2$	2.53×10^{13}	0	700
$HO_2 + H \rightarrow OH + OH$	5.40×10^{14}	0	1 800
$HO_2 + O \rightarrow OH + O_2$	5.00×10^{13}	0	1 000
$HO_2 + HO_2 \rightarrow H_2O_2 + O_2$	1.99×10^{12}	0	0
$HO_2 + H_2 \rightarrow H_2O_2 + H$	3.00×10^{11}	0	18 700
$H_2O_2 + OH \rightarrow HO_2 + H_2O$	1.02×10^{13}	0	1 900
$M + H_2O_2 \rightarrow OH + OH$	1.21×10^{17}	0	45 500

*The parameters A, n, and E refer to the Arrhenius equation, $k = AT^n e^{-E/RT}$. The rate coefficient k is in s^{-1} for unimolecular reactions, cm^3/mole-s for bimolecular reactions, and cm^6/$mole^2$-s for termolecular reactions. Activation energy E is in cal/mole.

same pressure served to encourage the comparison of the present data with a combined kinetic mechanism. The methane kinetic mechanism was combined with the silane-hydrogen mechanism of reference 4. The methane portion of the combined mechanism in table II was used to calculate the ignition delay time for methane without an ignition aid. The predictions for methane alone are shown by the upper solid line in figure 7.

The results of the numerical studies on the silane-methane reaction mechanism are given in figure 7 together with the corresponding experimental results designated by the dashed line. Comparing the experimental results with calculated results for methane without the silane reactions, clearly reveals that the presence of silane enhances the ignition of the methane; however, the enhancement is not as large as predicted with the combined silane-methane oxidation mechanism. The ignition delay times calculated with the combined mechanism are about an order of magnitude less than the measured value for a given temperature.

Examination of the calculated history of the various reactants and products during the ignition delay period reveals that the ignition of silane precedes the ignition of methane by 50 to 75 μs. This observation was apparent in the analytical results but not in the experimental results. The ignition of the methane is enhanced by the large amounts of free radicals that are produced during the ignition of silane. In the combined silane-methane oxidation mechanism, the methane oxidation mechanism and the silane oxidation mechanism are coupled only through the free radicals H, O, OH, and HO_2. A possible explanation for the difference between the calculated and experimental results is that some important reactions have been omitted, especially those that involve coupling between the silane and methane intermediates. In the methane reaction mechanism, the formation of ethane, C_2H_6, through the reaction

$$CH_3 + CH_3 \rightarrow C_2H_6$$

and the subsequent C_2H_6 reactions can be important. Analogous reactions involving the CH_3 and SiH_3 radicals, for example,

$$CH_3 + SiH_3 \rightarrow CH_3SiH_3$$

may occur in the silane-methane system. However, it is not intuitively obvious that these additional reaction paths would result in an order of magnitude change in the ignition delay time.

Another possible contributor to the differences between calculated and experimental results in figure 7 is the uncertainty in the silane oxidation reaction mechanism of reference 4 for the present test conditions. This mechanism was tested and refined by comparing the kinetic behavior observed in shock tube studies with that predicted by the mechanism. The rate coefficients for many reactions were unknown and had to be estimated. However, the mechanism was compared with experimental data for a lower temperature range (800 K to 1050 K) than in the present study. It is possible that the silane mechanism is inappropriate at the higher temperatures (1100 K to 1300 K) of the present silane-methane experiments. Until additional reaction rate data are obtained on silane oxidation at higher temperatures, this particular contributor to the difference between the calculated and experimental results cannot be identified.

Concluding Remarks

Ignition delay times in mixtures of methane, silane, and oxygen diluted with argon and nitrogen were measured behind reflected shock waves generated in the chemical kinetic shock tube at the Langley Research Center. Pressures of 1.25 atm and temperatures between 1100 K and 1300 K were generated behind the reflected shocks; these levels are representative of those occurring within a supersonic ramjet combustor. Expressions for ignition delay time as a function of temperature were obtained from least squares curve fits to the data for overall equivalence ratios ϕ of 0.7 and 1.0; these expressions are for argon as the diluent gas,

$$\tau = 3.95 \times 10^{-2}\, e^{11\,339/T_5} \quad \text{for } \phi = 0.7$$

$$\tau = 1.0 \times 10^{-3}\, e^{15\,732/T_5} \quad \text{for } \phi = 1.0$$

and for nitrogen as the diluent gas,

$$\tau = 6.83 \times 10^{-3}\, e^{12\,800/T_5} \quad \text{for } \phi = 0.7$$

$$\tau = 2.0 \times 10^{-4}\, e^{16\,944/T_5} \quad \text{for } \phi = 1.0$$

where τ is ignition delay time (in microseconds) and T_5 is temperature (Kelvin).

There was very little difference observed for the two equivalence ratios. Infrared wavelength observations at 4.38 μm for carbon dioxide indicated that the ignition of silane and methane occurred simultaneously (within the resolution of the measurements); however, the analytical model using a silane-methane reaction kinetic mechanism assembled for this comparison indicated that ignition of silane and methane occurred at different times (as much as 50 μs to 75 μs at the lower temperatures).

The combined chemical kinetic mechanism was assembled from a mechanism that accurately predicted

methane ignition and a mechanism that accurately predicted silane-hydrogen ignition. This kinetic mechanism was used to obtain a theoretical comparison for the silane-methane mixture. The combined mechanism predicted shorter ignition delay times than were actually obtained experimentally. Additional reactions, possibly between silyl and methyl fragments, are needed to develop a good silane-methane mechanism. Both the experiment and the assembled kinetic mechanism used for the theoretical comparison showed that the presence of silane significantly reduced ignition delay time.

NASA Langley Research Center
Hampton, VA 23665
January 2, 1985

References

1. Andrews, E. H.; Northam, G. B.; Torrence, M. G.; and Trexler, C. A.: Mach 4 Tests of a Hydrogen-Burning Airframe-Integrated Scramjet. *18th JANNAF Combustion Meeting, Volume IV*, Debra Sue Eggleston, ed., CPIA Publ. 347 (Contract N00024-81-C-5301), Appl. Phys. Lab., Johns Hopkins Univ., Oct. 1981, pp. 87–96.
2. Beach, H. Lee, Jr.; Mackley, Ernest A.; and Guy, Robert W.: *Mach 7 Tests of the Langley Airframe-Integrated Scramjet.* NASA TM-84595, 1983.
3. McLain, Allen G.; Jachimowski, Casimir J.; and Rogers, R. Clayton: *Ignition of* SiH_4-H_2-O_2-N_2 *Behind Reflected Shock Waves.* NASA TP-2114, 1983.
4. Jachimowski, Casimir J.; and McLain, Allen G.: *A Chemical Kinetic Mechanism for the Ignition of Silane/Hydrogen Mixtures.* NASA TP-2129, 1983.
5. McLain, Allen G.; and Rao, C. S. R.: *A Hybrid Computer Program for Rapidly Solving Flowing or Static Chemical Kinetic Problems Involving Many Chemical Species.* NASA TM X-3403, 1976.
6. Westbrook, Charles K.: An Analytical Study of the Shock Tube Ignition of Mixtures of Methane and Ethane. *Combust. Sci. & Technol.*, vol. 20, nos. 1 & 2, 1979, pp. 5–17.
7. Frenklach, Michael; and Bornside, David E.: Shock-Initiated Ignition in Methane-Propane Mixtures. *Combust. & Flame*, vol. 56, no. 1, Apr. 1984, pp. 1–27.

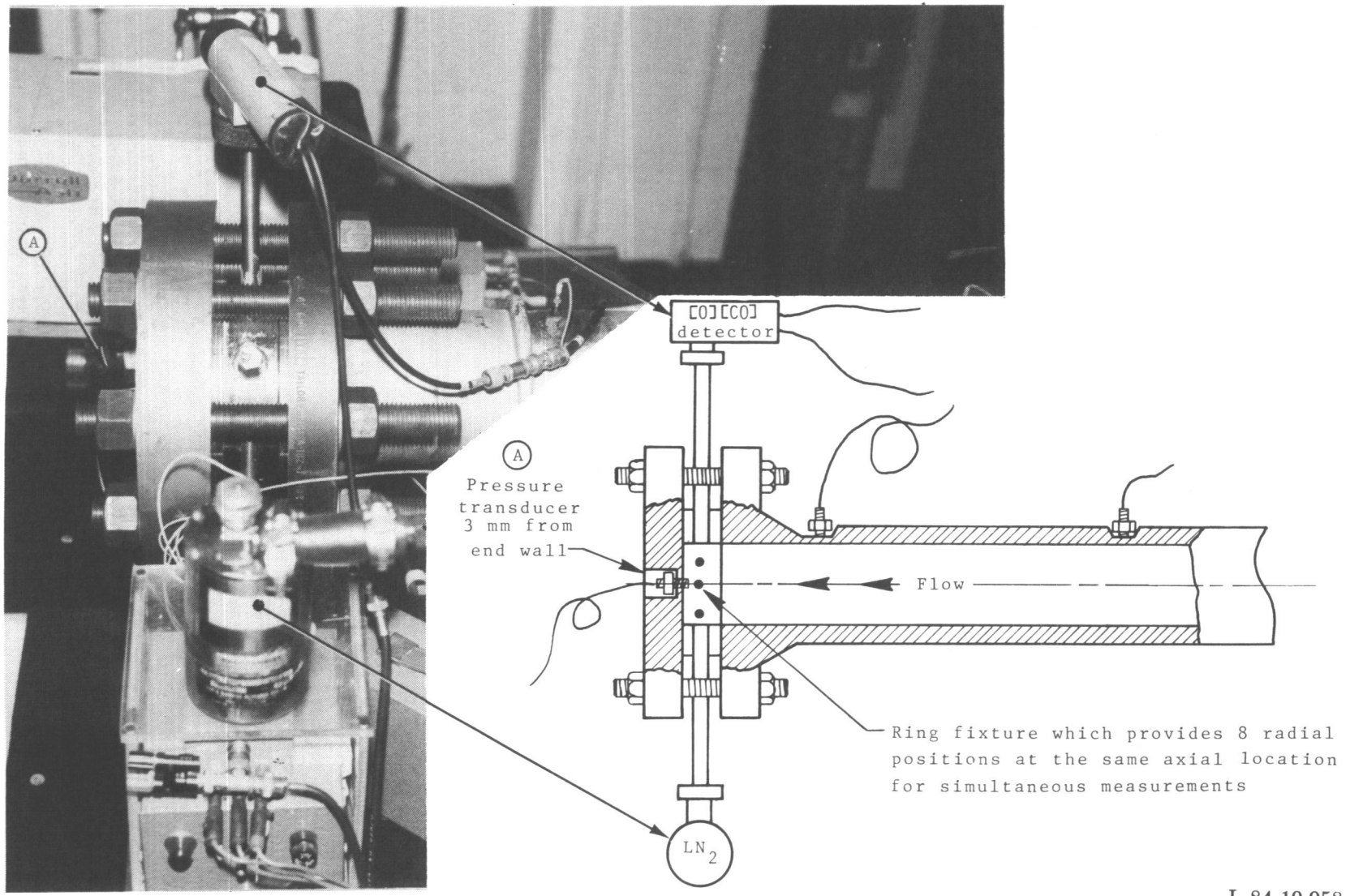

L-84-10,958

Figure 1. Photograph and schematic diagram of ring fixture and instrumentation arrangement.

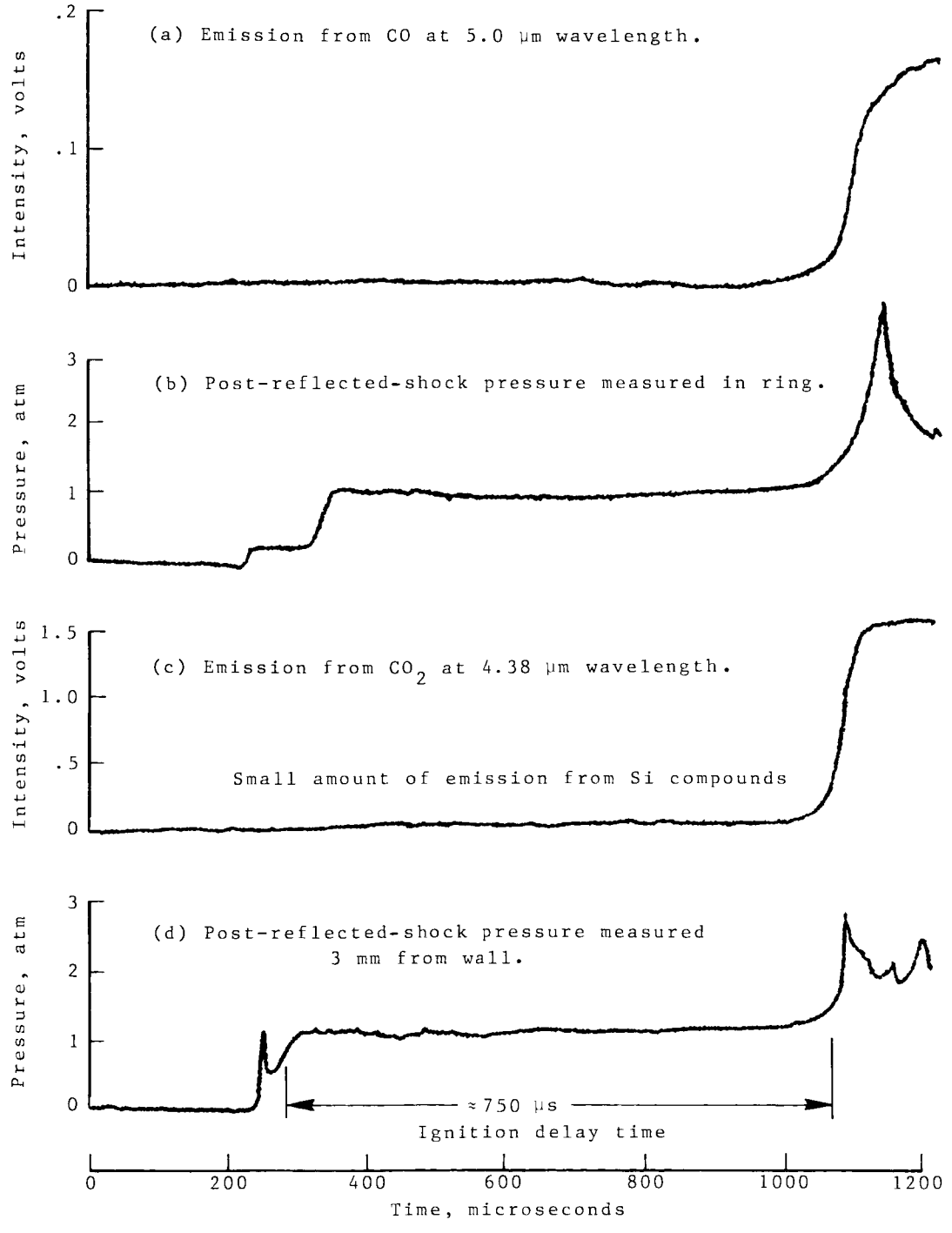

Figure 2. Reproduction of pressure and emission sensor outputs recorded by a digital processing oscilloscope.

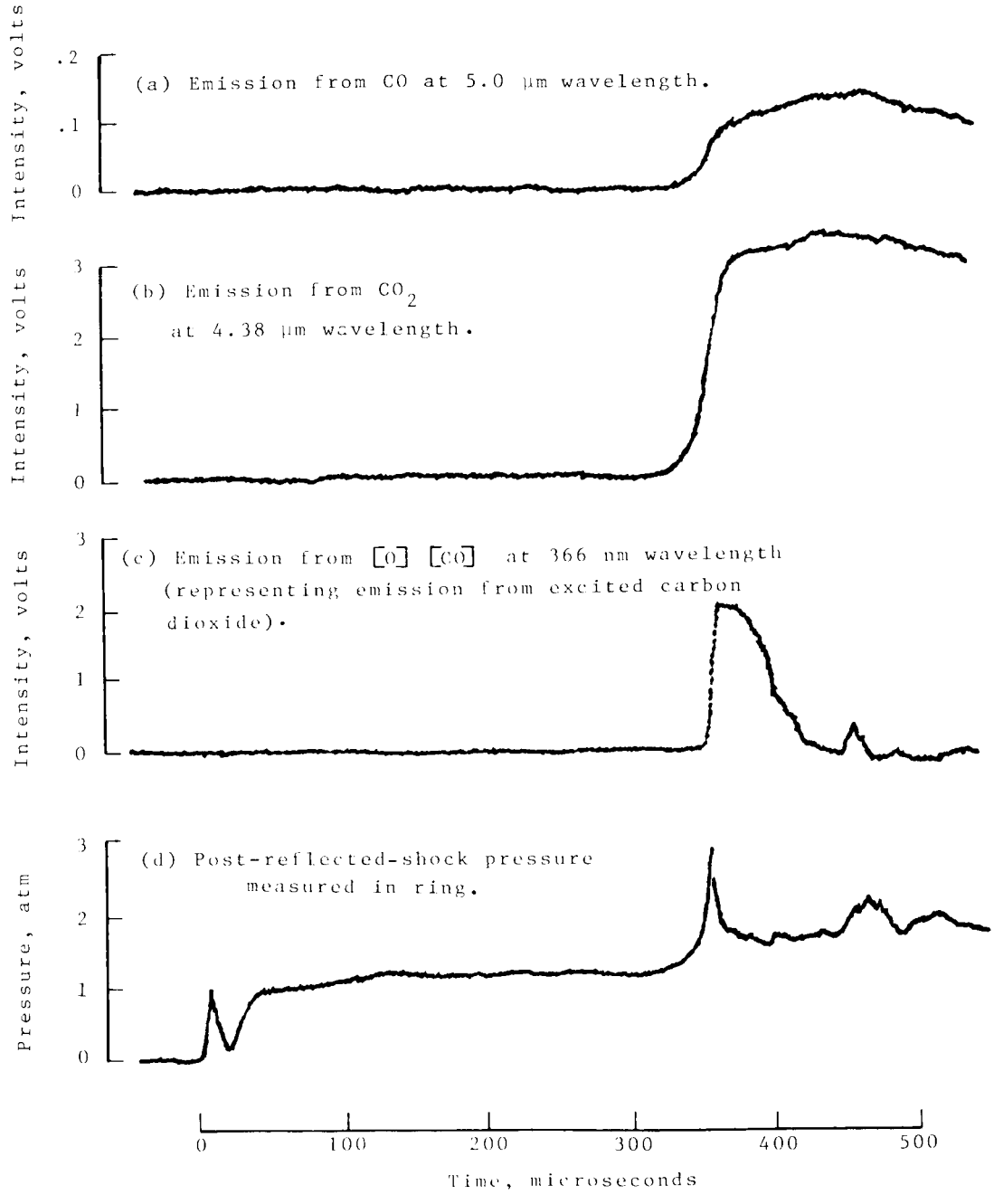

Figure 3. Reproduction of a digital recording of emission occurring at several wavelengths accompanied by a rapid pressure increase. Recordings were made radially at the same axial location in the test tube.

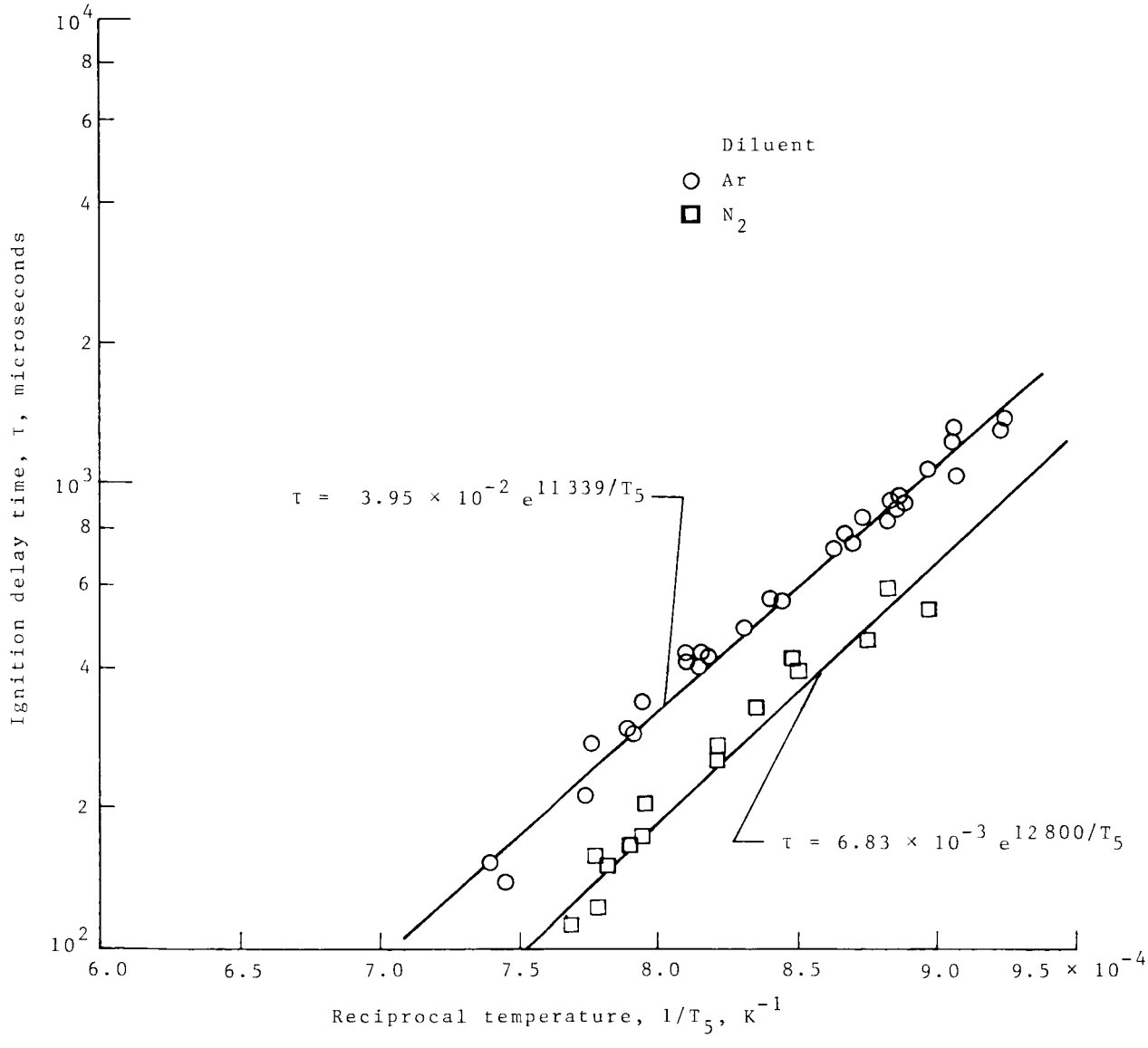

Figure 4. Variation of ignition delay time with reciprocal temperature (at frozen reflected shock conditions) for an overall equivalence ratio of 0.70.

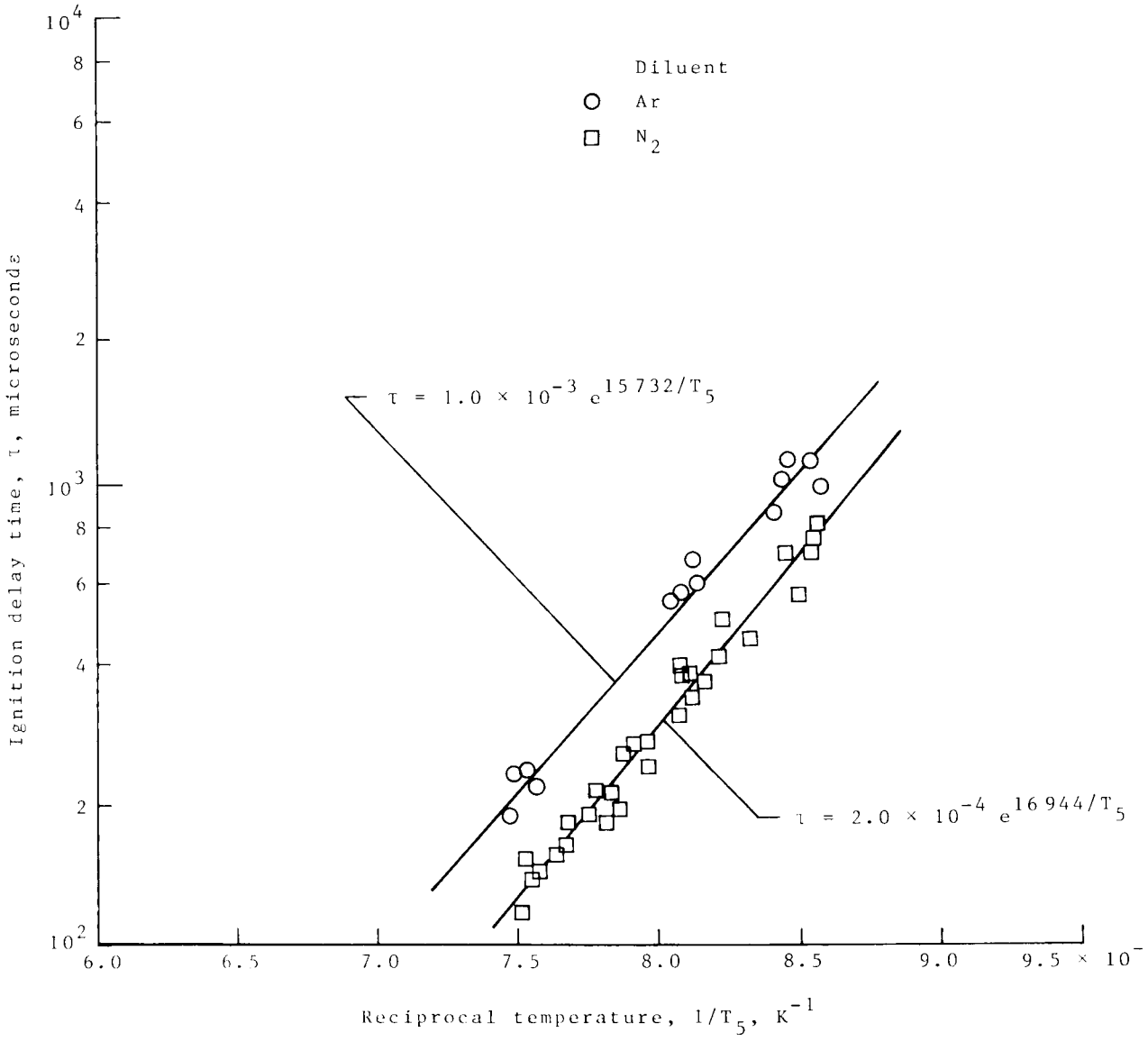

Figure 5. Variation of ignition delay time with reciprocal temperature (at frozen reflected shock conditions) for an overall equivalence ratio of 1.0.

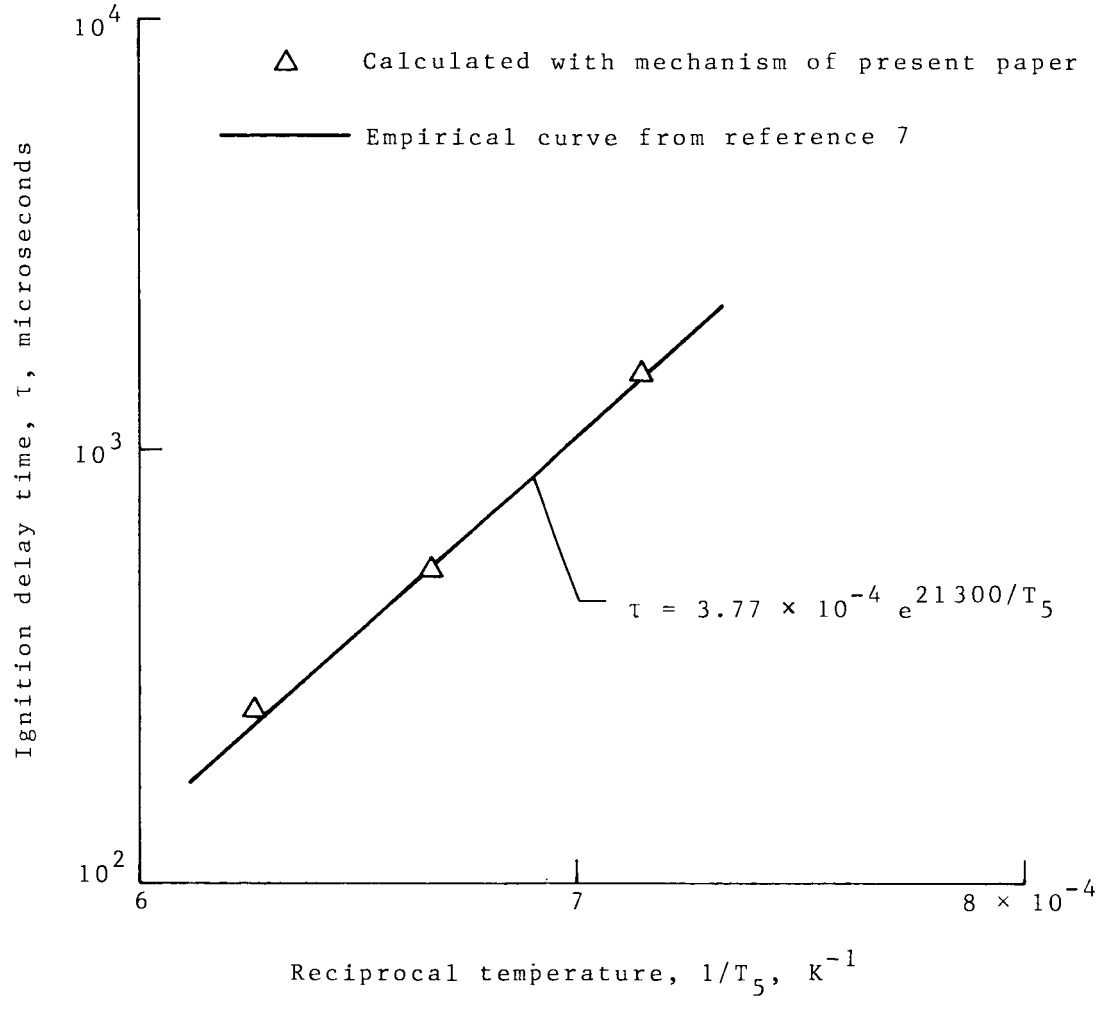

Figure 6. Comparison between ignition delay times calculated from the kinetic mechanism assembled for the present paper and from the empirical curve from reference 7. For a mixture of 9.5% CH_4–19.0% O_2–71.5% Ar, and a pressure of 2.5 atm.

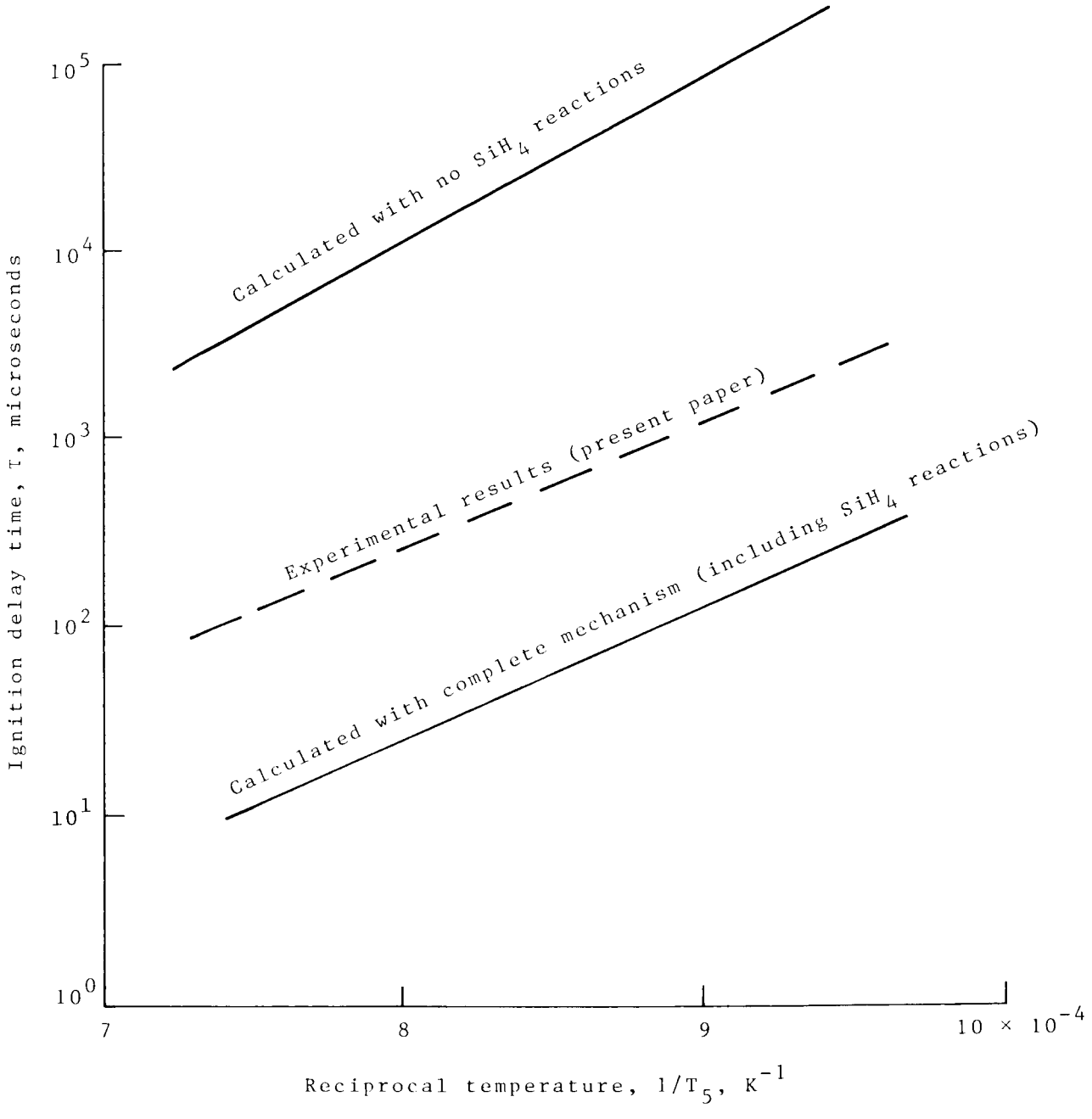

Figure 7. Comparison between calculated and measured ignition delay times for the mixture of 8.4% CH_4–2.1% SiH_4–21.0% O_2–68.5% Ar, and a pressure of 1.25 atm.

1. Report No.	2. Government Accession No.	3. Recipient's Catalog No.
NASA TP-2415		

4. Title and Subtitle	5. Report Date
Ignition of Mixtures of SiH_4, CH_4, O_2, and Ar or N_2 Behind Reflected Shock Waves	April 1985
	6. Performing Organization Code: 505-43-83-03
7. Author(s): Allen G. McLain, Casimir J. Jachimowski, and R. Clayton Rogers	8. Performing Organization Report No.: L-15881
9. Performing Organization Name and Address: NASA Langley Research Center, Hampton, VA 23665	10. Work Unit No.
	11. Contract or Grant No.
12. Sponsoring Agency Name and Address: National Aeronautics and Space Administration, Washington, DC 20546	13. Type of Report and Period Covered: Technical Paper
	14. Sponsoring Agency Code

15. Supplementary Notes

16. Abstract

Ignition delay times in mixtures of methane, silane, and oxygen diluted with argon and nitrogen were measured behind reflected shock waves generated in the chemical kinetic shock tube at Langley Research Center. The delay times were inferred from the rapid increase in pressure that occurs at ignition, and the ignition of methane was verified from the emission of infrared radiation from carbon dioxide. Pressures of 1.25 atm and temperatures from 1100 K to 1300 K were generated behind the reflected shocks; these levels are representative of those occurring within a supersonic ramjet combustor. Expressions for the ignition delay time as a function of temperature were obtained from least squares curve fits to the data for overall equivalence ratios of 0.7 and 1.0. The ignition delay times with argon as the diluent were longer than those with nitrogen as the diluent. The infrared wavelength observations at 4.38 μm for carbon dioxide indicated that silane and methane ignited simultaneously (i.e., within the time resolution of the measurement). A combined chemical kinetic mechanism for mixtures of silane, methane, oxygen, and argon or nitrogen was assembled from one mechanism that accurately predicted the ignition of methane and a second mechanism that accurately predicted silane-hydrogen ignition. Comparisons between this combined mechanism and experiment indicated that additional reactions, possibly between silyl and methyl fragments, are needed to develop a good silane-methane mechanism.

17. Key Words (Suggested by Authors(s))
Ignition in shock tube
Silane
Methane
Kinetic mechanism

18. Distribution Statement
Unclassified - Unlimited

Subject Category 07

19. Security Classif.(of this report)	20. Security Classif.(of this page)	21. No. of Pages	22. Price
Unclassified	Unclassified	15	A02

For sale by the National Technical Information Service, Springfield, Virginia 22161

NASA-Langley, 1985